Demonstration of a HeNe/CH_4-based optical molecular clock

Seth M. Foreman, Adela Marian, and Jun Ye

JILA, National Institute of Standards and Technology and University of Colorado, Boulder, Colorado 80309-0440

Evgeny A. Petrukhin and Mikhail A. Gubin

P. N. Lebedev Physical Institute, 53 Leninskiy Prospekt, 119991 Moscow, Russia

Oliver D. Mücke, Franco N. C. Wong, Erich P. Ippen, and Franz X. Kärtner

Department of Electrical Engineering and Computer Science, Research Laboratory of Electronics, Massachusetts Institute of Technology, Cambridge, Massachusetts 02139-4307

Received September 23, 2004

We implement a simple optical clock based on the $F_2^{(2)}$ $[P(7), \nu_3]$ optical transition in methane. A single femtosecond laser's frequency comb undergoes difference frequency generation to provide an IR comb at 3.39 μm with a null carrier-envelope offset. This IR comb provides a phase-coherent link between the 88-THz optical reference and the rf repetition rate. Comparison of the repetition rate signal with a second femtosecond comb stabilized to molecular iodine shows an instability of 1.2×10^{-13} at 1 s, limited by microwave detection of the repetition rates. The single-sideband phase noise of the microwave signal, normalized to a carrier frequency of 1 GHz, is below -93 dBc/Hz at 1-Hz offset.

OCIS codes: 120.3940, 320.7160, 190.7110.

Optical frequency combs based on femtosecond lasers have become a powerful tool for frequency metrology, allowing phase-coherent links to be established in the electromagnetic spectrum spanning from visible to microwave frequencies.[1] The optical frequencies ν_m of a femtosecond comb are related to two radio frequencies: f_{rep}, the repetition frequency of the pulse train, and f_0, the carrier-envelope offset frequency. The relationship $\nu_m = mf_{\text{rep}} + f_0$, where integer m is $\sim 10^6$, allows optical-microwave phase coherence to be achieved in a single step when controlling the comb's two degrees of freedom.[1]

To establish an optical clock, one needs to derive an f_{rep} phase coherently from an optical frequency standard ν_s. A heterodyne beat signal f_b between ν_s and ν_m is used to establish a connection between ν_s and f_{rep}, provided that f_0 is either independently stabilized or eliminated as a variable.[2,3] Various schemes have been employed, the most common of which involves the use of self-referencing to detect and stabilize f_0.[4] This technique is most easily implemented with an octave-spanning spectral bandwidth, which is usually achieved through spectral broadening in a microstructure or tapered fiber. More recently, lasers that directly emit octave-spanning spectra[5,6] have made possible the elimination of such highly nonlinear fibers from the clockwork while maintaining a stable f_0 lock. A second scheme involves orthogonalizing error signals derived from two optical heterodyne beats of the comb against a reference laser (ν_s) and its second harmonic ($2\nu_s$).[3] If the two optical beats are expressed as $f_{b1} = \nu_s - (mf_{\text{rep}} + f_0)$ and $f_{b2} = 2\nu_s - (2mf_{\text{rep}} + f_0)$, then the difference between the two beats is $f_{b2} - f_{b1} = \nu_s - mf_{\text{rep}}$, permitting control of f_{rep} from ν_s without stabilizing f_0. To avoid the use of highly nonlinear fiber or the need for special octave-spanning lasers, Amy-Klein *et al.*[7] locked two modes of the same femtosecond comb to two cw diode lasers. The difference frequency between the two cw lasers was locked to a stable infrared reference. This technique is insensitive to f_0 but involves numerous locks and lasers. Here we demonstrate the operation of an optical molecular clock based on difference-frequency generation (DFG) that does not rely on microstructure fiber, additional cw lasers, or any stabilization of f_0.[8,9] A HeNe laser operating at 3.39 μm is stabilized by the methane $F_2^{(2)}$ line and serves as an infrared optical frequency standard to which f_{rep} of a custom-designed Ti:sapphire laser is phase-coherently stabilized. We note that the DFG approach has also been carried out between two independent but synchronized femtosecond combs.[10]

Our setup is similar to that described in Fig. 1 of Ref. 9. A prismless mode-locked Ti:sapphire laser outputs 150 mW of average power at $f_{\text{rep}} = 78$ MHz when pumped with 6.5 W of 532-nm light. Because of a uniquely designed output coupler,[9] the output spectrum exhibits spectral peaks at 670 and 834 nm, shown in Fig. 1(a), which have a frequency difference corresponding to the 3.39-μm wavelength. A third parasitic peak at $\sim$902 nm is not used in the experiment. Approximately 12.3 mW of average power is contained within the 7-nm FWHM bandwidth of the 670-nm peak, and a 10-nm-wide spectral region centered at 831 nm has 7.8 mW of average power. The Ti:sapphire output is focused into a temperature-controlled periodically poled lithium niobate (PPLN) crystal.[9] For efficient DFG inside the PPLN the Ti:sapphire beam traverses a prism-based delay line placed before the PPLN for an optimal temporal overlap of the 670- and 834-nm spectral components. The resultant offset-free IR frequency comb passes through a 50-nm FWHM bandwidth interference filter centered at 3.39 μm and transmits $\sim$10 μW of average power, corresponding to nearly 600 pW per mode of the IR comb. With an IR monochromator and lock-in detection we observe that the IR comb has a bandwidth of $\sim$270 nm (7 THz) centered near 3.4 μm

0146-9592/05/050570-03$15.00/0

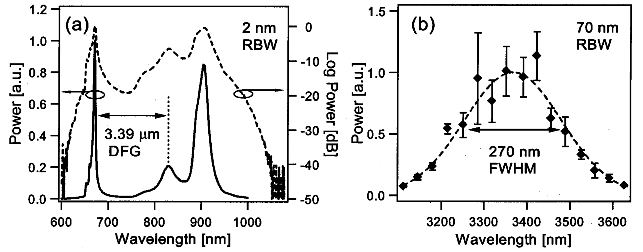

Fig. 1. Spectra of (a) direct Ti:sapphire laser output and (b) IR comb generated by difference-frequency mixing of the Ti:sapphire laser comb in a PPLN crystal. RBW, resolution bandwidth.

(88.5 THz) as shown in Fig. 1(b). Note that frequency modes ν_n of the IR comb are expressed in terms of two modes $\nu_{m'}$ and $\nu_{m''}$ of the original Ti:sapphire comb as $\nu_n = \nu_{m'} - \nu_{m''} = (m' f_{\mathrm{rep}} + f_0) - (m'' f_{\mathrm{rep}} + f_0) = n f_{\mathrm{rep}}$, where integer $n = m' - m''$. We emphasize that the IR comb's modes have no dependence on f_0.[8]

The optical frequency standard is a compact, portable, double-mode HeNe laser stabilized to resonances of the $F_2{}^{(2)}$ transition in methane (HWHM ~ 200 kHz, hyperfine structure is unresolved) at 3.39 μm. Saturated absorption and saturated dispersion resonances are both used to lock the reference laser frequency, providing optical radiation with a linewidth of <100 Hz. This type of reference HeNe laser is being routinely incorporated in transportable HeNe/CH_4 systems with telescopic beam expanders for providing resolution of methane's hyperfine structure and frequency repeatability of 2×10^{-13} over several years.[11] Measurements with a frequency chain indicate an instability at 1 s of $<4 \times 10^{-13}$, limited by a hydrogen maser. A direct optical comparison of two versions of the system (one was a nontransportable, resolved hyperfine-structure version) has a demonstrated Allan deviation of $\sim 2 \times 10^{-14}$ at 1 s. A second HeNe laser (heterodyne laser) is phase locked to the reference laser with a fixed ~600-kHz frequency offset and provides the optical field we use to stabilize our IR comb. An amplifier HeNe tube was used to increase the beam's power from 300 μW to ~1 mW.

After the cw HeNe beam and IR comb were combined on a 60/40 beam splitter, they passed through a 50-nm FWHM interference filter centered at 3.39 μm. A 1.8-cm focal-length CaF_2 lens focused the beams onto a liquid-nitrogen-cooled InSb photodiode with a 250-μm-diameter active area. A heterodyne beat between the cw HeNe beam at ν_{HeNe} and the Nth line of the IR comb was detected and amplified. As shown in Fig. 2, beat frequency $f_b = N f_{\mathrm{rep}} - \nu_{\mathrm{HeNe}}$ has a signal-to-noise ratio of 25 dB in a 100-kHz bandwidth. It is subsequently phase locked by means of a rf tracking oscillator to a 70-MHz synthesized signal (with a negligible noise contribution) derived from a stable cesium reference. Control of f_b is achieved by feedback of the phase-locked loop error signal to a piston-mode piezoelectric transducer on which the Ti:sapphire laser's fold mirror was mounted. Now rf frequency f_{rep} is directly expressed in terms of optical frequency ν_{HeNe} as $f_{\mathrm{rep}} = (\nu_{\mathrm{HeNe}} + 70\ \mathrm{MHz})/N$. The optical clock signals (f_{rep}) are independently detected at the beam splitter's second port.

The rf clock signal's stability was compared with both a hydrogen maser and the repetition frequency of a second Ti:sapphire laser operating as part of an optical clock based on a molecular iodine transition.[3] For comparison with the maser, the tenth harmonic of f_{rep} was compared with a 780-MHz signal derived from the National Institute of Standards and Technology (NIST) ST-22 hydrogen maser and transferred to JILA through a single-mode fiber.[12] The I_2 clock consists of a second Ti:sapphire laser with a 100-MHz repetition rate. Its frequency comb was fixed by locking f_0 by use of self-referencing and by phase locking one comb line near 1064 nm to a Nd:YAG laser that was stabilized to molecular iodine.[3] The seventh harmonic of this I_2-referenced Ti:sapphire laser's f_{rep} is compared with the ninth harmonic of the CH_4-referenced Ti:sapphire laser's f_{rep} at ~702 MHz. We deliberately introduce an offset frequency of 10 kHz between the two stabilized f_{rep} harmonics. A double-balanced mixer detects this 10-kHz difference frequency that is subsequently filtered and counted with a 1-s gate time to determine the Allan deviation of the CH_4 clock compared with the maser or the I_2 clock.

Figure 3(a) shows representative frequency counting for both comparisons. Denoting the comparison frequency (780 MHz for the maser, 702 MHz for the I_2 clock) as f_c, frequency fluctuations Δf_c were

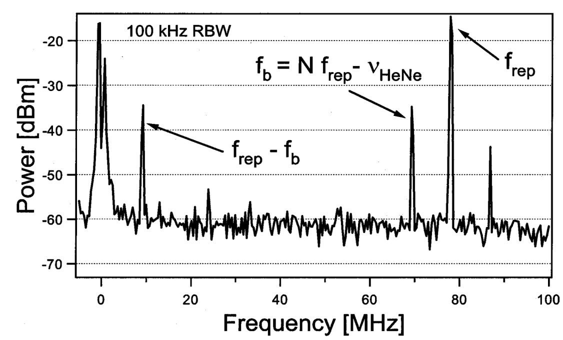

Fig. 2. Heterodyne beats between the CH_4-stabilized HeNe laser and neighboring IR comb components, with a signal-to-noise ratio of >25 dB in a 100-kHz RBW.

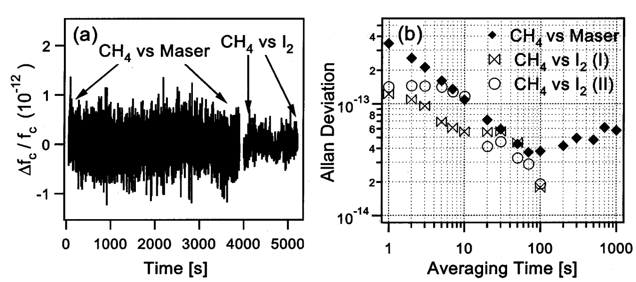

Fig. 3. Comparison of the rf signal from the CH_4 clock with NIST's hydrogen maser and with the I_2 clock's rf signal. (a) Fractional fluctuations of the comparison frequency in each case. (b) Allan deviations for comparison with the maser (diamonds), the I_2 clock with fiber-coupled detection of f_{rep} (circles), and the I_2 clock with free-space-coupled detection of f_{rep} (bow ties).

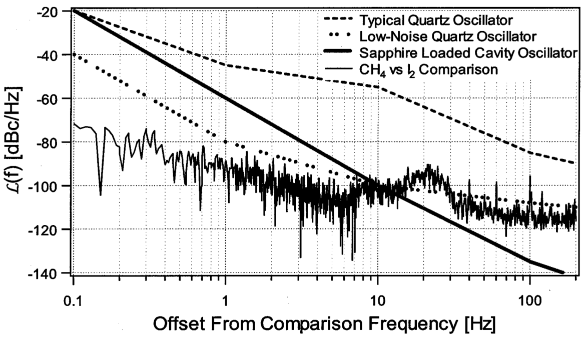

Fig. 4. SSB phase noise of the CH_4 clock signal when compared with the I_2 clock signal. Additional curves show the approximate SSB phase noise of extremely low-phase-noise microwave sources for comparison. All data were scaled for a 1-GHz carrier.

normalized to f_c for fair evaluation of the two stability measurements. Parasitic backreflections from surfaces inside the HeNe resonator shift the centers of the saturated absorption and saturated dispersion resonances of the reference system.[13] As the position of the reflecting surface moved because of temperature changes, both a slow drift and a slow oscillation of ν_{HeNe} were observed. A quadratic drift of Δf_c tightly correlated with recorded temperature changes of the HeNe system was subtracted from the raw data. An oscillation with a period of >20 s is still present, however. Figure 3(b) shows the Allan deviations determined from various frequency-counting records. Measurements against the maser (filled diamonds) were limited by the maser's intrinsic short-term instability of $\sim 3 \times 10^{-13}$ at 1 s. Data run I (bow ties) against the I_2 clock used free-space photodiodes for detection of both clocks' repetition rates, whereas data run II (circles) used fiber-coupled detectors that exhibit greater phase noise and amplitude-phase conversion. The noisy plateau in the Allan deviation for data run II for $\tau < 20$ s strongly suggests that amplitude-phase conversion in the detection process limits our instability for short time scales.[14] However, for time scales of $20\ \mathrm{s} < \tau < 100$ s, data run II exhibits stability comparable with data run I, even though they were taken under very different conditions of temperature fluctuations in the laboratory. Therefore the instability of our CH_2 clock as compared with the I_2 clock is $\sim 1.2 \times 10^{-13}$ at 1 s, averaging down as $\tau^{-1/2}$ for $\tau < 100$ s, limited by excess noise in the photodetection process.

To characterize the phase noise of our CH_4 clock signal, we examined the 10-kHz signal derived from comparison with the I_2 clock (using free-space detection of the clock signals) with a fast Fourier transform spectrum analyzer. These measurements represent an upper limit to the single-sideband (SSB) phase noise, because they are sensitive to amplitude noise as well. Figure 4 shows our measurement results after scaling the phase noise up to a 1-GHz carrier frequency for ease of comparison against other oscillators. We include curves representing the typical SSB phase noise of other extremely stable microwave sources.[15] Less than 10 Hz from the carrier, our SSB phase noise is superior to some of the lowest-phase-noise microwave sources available, achieving −93 dBc/Hz at a 1-Hz offset. The rf amplifiers limit the system's SSB noise.

Without the need for stabilization of f_0 and coupled with the use of a portable highly stable $HeNe/CH_4$ optical standard, our setup represents a compact, reliable clock with high stability and exceedingly low phase noise, which can in principle be operated for long (>24-h) periods. We also note the applicability of our scheme to absolute frequency measurements throughout the near- and mid-IR spectral range.

This research has been supported by the U.S. Office of Naval Research, NIST, and NASA. It was also supported in part by the Russian Foundation for Basic Research and the research program Femtosecond Optics administered by the Russian Academy of Sciences. O. D. Mücke acknowledges support from the Alexander von Humboldt Foundation. S. M. Foreman's e-mail address is foreman@colorado.edu.

References

1. J. Ye, H. Schnatz, and L. W. Hollberg, IEEE J. Sel. Top. Quantum Electron. **9,** 1041 (2003).
2. S. A. Diddams, T. Udem, J. C. Bergquist, E. A. Curtis, R. E. Drullinger, L. Hollberg, W. M. Itano, W. D. Lee, C. W. Oates, K. R. Vogel, and D. J. Wineland, Science **293,** 825 (2001).
3. J. Ye, L. S. Ma, and J. L. Hall, Phys. Rev. Lett. **87,** 270801 (2001).
4. D. J. Jones, S. A. Diddams, J. K. Ranka, A. Stentz, R. S. Windeler, J. L. Hall, and S. T. Cundiff, Science **288,** 635 (2000).
5. T. M. Fortier, D. J. Jones, and S. T. Cundiff, Opt. Lett. **28,** 2198 (2003).
6. L. Matos, D. Kleppner, O. Kuzucu, T. R. Schibli, J. Kim, E. P. Ippen, and F. X. Kaertner, Opt. Lett. **29,** 1683 (2004).
7. A. Amy-Klein, A. Goncharov, C. Daussy, C. Grain, O. Lopez, G. Santarelli, and C. Chardonnet, Appl. Phys. B **78,** 25 (2004).
8. M. Zimmermann, C. Gohle, R. Holzwarth, T. Udem, and T. W. Hänsch, Opt. Lett. **29,** 310 (2004).
9. O. D. Mücke, O. Kuzucu, F. N. C. Wong, E. P. Ippen, F. X. Kärtner, S. M. Foreman, D. J. Jones, L.-S. Ma, J. L. Hall, and J. Ye, Opt. Lett. **29,** 2806 (2004).
10. S. M. Foreman, D. J. Jones, and J. Ye, Opt. Lett. **28,** 370 (2003).
11. M. A. Gubin, D. A. Tyurikov, A. S. Shelkovnikov, E. V. Koval'chuk, G. Kramer, and B. Lipphardt, IEEE J. Quantum Electron. **31,** 2177 (1995).
12. J. Ye, J.-L. Peng, R. J. Jones, K. W. Holman, J. L. Hall, D. J. Jones, S. A. Diddams, J. Kitching, S. Bize, J. C. Bergquist, L. W. Hollberg, L. Robertsson, and L.-S. Ma, J. Opt. Soc. Am. B **20,** 1459 (2003).
13. D. D. Krylova, A. S. Shelkovnikov, E. A. Petrukhin, and M. A. Gubin, Quantum Electron. **34,** 554 (2004).
14. E. N. Ivanov, S. A. Diddams, and L. Hollberg, IEEE J. Sel. Top. Quantum Electron. **9,** 1059 (2003).
15. Poseidon Scientific Instruments sapphire loaded cavity oscillator and Frequency Electronics, Inc., FE-102A-100 and FE-205A. Mention of commercial product names is for technical communication only.